

Probing nonlinear mechanical effects through electronic currents: the case of a nanomechanical resonator acting as electronic transistor

A. Nocera^{1,2}, C.A. Perroni^{3,4}, V. Marigliano Ramaglia^{1,4} and V. Cataudella^{3,4}

¹CNISM, ²Dipartimento di Fisica E. Amaldi, Università di Roma Tre,
Via della Vasca Navale 84, I-00146 Roma, Italy

³CNR-SPIN, ⁴Università degli Studi di Napoli Federico II,
Complesso Universitario Monte Sant'Angelo, Via Cintia, I-80126 Napoli, Italy.

We study a general model describing a self-detecting single electron transistor realized by a suspended carbon nanotube actuated by a nearby antenna. The main features of the device, recently observed in a number of experiments, are accurately reproduced. When the device is in a low current-carrying state, a peak in the current signals a mechanical resonance. On the contrary, a dip in the current is found in high current-carrying states. In the nonlinear vibration regime of the resonator, we are able to reproduce quantitatively the characteristic asymmetric shape of the current-frequency curves. We show that the nonlinear effects coming out at high values of the antenna amplitude are related to the effective nonlinear force induced by the electronic flow. The interplay between electronic and mechanical degrees of freedom is understood in terms of an unifying model including in an intrinsic way the nonlinear effects driven by the external probe.

I. INTRODUCTION

It has been recently shown that carbon nanotubes can act simultaneously as single electron transistors¹ (SET) and as nanoelectromechanical systems (NEMS)^{2,3}. The idea is to use a single carbon nanotube placed between two metal contacts in a suspended configuration as a self-detecting SET. Due to the extreme properties of carbon nanotubes (ideal for NEMS applications, because they have a low mass and a high Young's modulus), the electronic current flowing through the device results very sensitive to the dynamics of the nanotube itself.

Although the main effort has been focused on detecting the quantum regime of mechanical resonators⁴⁻⁶, recently, G. A. Steele *et al.*⁷ and A. K. Huttel *et al.*⁸ were able to fabricate a carbon nanotube electromechanical device working in the semiclassical regime (resonator frequencies in MHz range compared to an electronic hopping frequency of the order of tens of GHz) with an extremely large quality factor ($Q > 10^5$). By measuring the variations of the electronic current flowing through the nanotube as function of the frequency of a nearby antenna actuating its motion, they were able to detect very well defined resonances corresponding to the bending mode of the nanotube itself. The possibility of using currents to probe nanomechanical resonances is strongly related to the extremely large quality factor obtained. In particular, when the SET is in a low current-carrying state (far from electronic resonance), a peak in the current signals a mechanical resonance, while a dip is observed in a high current-carrying state (SET in electronic resonance). Moreover, by adjusting the antenna power, the nanotube resonator can easily be tuned into the nonlinear vibration regime. For small antenna amplitudes, the current-frequency curves are very well fitted by a Lorentzian, while a characteristic triangular shape or even hysteresis for large antenna amplitudes is obtained. Interestingly, the operating temperature can af-

fect the nonlinearity and the quality factor of the resonator in a non expected way: the nonlinear effects in current-frequency curves are washed out increasing the temperature⁹. A detailed analysis of a single frequency resonance dip has also shown that a broadening can be obtained increasing the source-drain voltage⁷. In Ref. 7, the authors were able to provide an explanation of some of the observed effects in terms of a model in which the gate voltage acquires an assigned time dependence. Within this phenomenological model, the back-action of the nanotube motion on detected current is understood neglecting completely the dynamics of the resonator and analyzing the problem directly at mechanical resonance conditions only in the limit of small external antenna amplitudes (linear response regime).

In this paper, we do not consider a priori assumptions on the resonator (nanotube) dynamics. Actually, in the device investigated in Ref. 7 and 8, the chemical potentials of the leads, to which the nanotube is anchored, differ by the value of the applied transport voltage eV_{bias} (where e is the electron charge), and thus the environment that the nanotube experiences cannot be considered at equilibrium since the voltages applied in the experiment are typically greater than the temperature, $eV_{bias} \gg k_B T$ (k_B being Boltzmann constant). Therefore, in order to understand the behavior of the device under such conditions, one needs to determine self-consistently the influence of electrical current and of the external antenna on the resonator dynamics, and vice versa, the influence of nonthermal nanotube vibrations driven by the antenna on the electronic current¹⁰. As rigorously demonstrated by Mozyrsky *et al.*¹¹, and re-obtained by us in a different way¹², in absence of the external antenna, the vibrational dynamics of the nanotube can be described, employing a separation between slow vibrational and fast electronic time scales¹²⁻¹⁵, by a Langevin equation¹⁴⁻¹⁹. This equation is ruled by an effective force as well as a damping and diffusive terms stemming from the interaction of the resonator with the

electronic bath consisting of both the nanotube itself (that can be described by a single electronic level¹⁶) and the out-of-equilibrium environment given by the macroscopic leads. By including the external antenna effects through a forcing term in the Langevin equation, we provide such a self-consistent description of vibrational and electronic dynamics as argued above.

A theoretical treatment of the nanotube based device investigated in 7 and 8, including the external antenna effects, has been already considered by G. Labadze and Ya. M. Blanter²⁰. In Ref. 20, the authors use a Fokker-Plank equation for the resonator distribution probability based on master equations^{21–25}. This approach implicitly assumes that the energy scale of the applied voltages is much larger than the electronic tunneling energy scale $\hbar\Gamma$, $eV_{bias} \gg \hbar\Gamma$. Moreover, tunneling is considered in the *sequential* regime and quantum effects in the electronic dynamics such as *cotunneling* are disregarded²⁶. We point out that these effects can be important to interpret the experimental results obtained by G. A. Steele *et al.*⁷ and A. K. Huttel *et al.*⁸ since, as already emphasized by G. Weick *et al.*¹⁶, the temperature is much smaller than $\hbar\Gamma$ and the bias voltage *effectively* applied to the electronic level of the nanotube can be less than or of the same order of magnitude of the electronic tunneling energy, $k_B T \ll eV_{bias}^{eff} \leq \hbar\Gamma$ ²⁷. Our approach, based on an adiabatic expansion of the time-dependent electronic Green function on the Keldysh contour in the small parameter ω_0/Γ ^{12–15}, takes into account from the beginning of all higher order terms in the tunneling matrix element between the leads and the nanotube (so sequential tunneling and cotunneling regimes are described in a unified way).

The inclusion of the external antenna effects in the effective Langevin equation for the resonator has allowed us to explore also the nonlinear response regime in a nonperturbative way. We point out that, even describing the vibrational dynamics of the nanotube as a single *harmonic* vibrational mode, we are able to reproduce all the main features observed in Ref. 7 and 8 including the nonlinear effects. Indeed, in the nonlinear vibration regime of the resonator, we are able to reproduce quantitatively the characteristic asymmetric shape of the current-frequency curves. The observed nonlinearity is due to the intrinsic nonlinear terms of the effective force stemming from the strong interaction between electron and resonator dynamics^{11,12,17–19}. These terms are completely neglected in Ref. 20, losing any possibility to describe renormalization frequency effects and to explore the nonlinear response regime for the resonator. We show that nonlinear effects can be highlighted *only dynamically* by applying large external antenna amplitudes. In this sense, our approach is different from other theoretical studies where nonlinear terms are discussed only statically⁷ or are added from the beginning assuming that the resonator is characterized by anharmonic terms.^{16,25,28}

Within our approach, the experimental results ob-

tained in Ref. 7 and 8 in the linear response regime are also reproduced, as well as the broadening of the mechanical resonance dip as function of the applied bias voltage. Furthermore, we are able to predict, in the limit of large bias, the onset of a fine double dip structure that could be experimentally observed.

The paper is organized as follows: In Sec. II we present the model able to describe the electronic transistor consisting of the vibrating nanotube. The equation of motion describing the resonator dynamics including the external antenna effects is also discussed. In Sec. III we present numerical results.

II. MODEL AND METHOD

We describe the suspended carbon nanotube with a single impurity Holstein model²⁹, that is able to catch the main physical ingredients of the experiments in Ref. 7 and 8. For the sake of clarity, we here point out that the model used in^{7,8} and in other papers in the literature^{20–23,25,30}, based on a capacitive coupling of the nanotube (dot) to the gate electrode, is equivalent to a Holstein-like coupling between the occupation on the dot and the vibrational degree of freedom (see Appendix A).

As suggested by Weick *et al.* [25], in the small energy window of interest for a single dip feature, the electronic part of the device is modeled as a single electronic level coupled to the leads through standard tunneling terms.

The electronic Hamiltonian is given by

$$\hat{\mathcal{H}}_{el} = V_{gate}^{eff} \hat{d}^\dagger \hat{d} + \sum_{k,\alpha} (V_{k,\alpha} \hat{c}_{k,\alpha}^\dagger \hat{d} + h.c.) + \sum_{k,\alpha} \varepsilon_{k,\alpha} \hat{c}_{k,\alpha}^\dagger \hat{c}_{k,\alpha}, \quad (1)$$

where nanotube's electronic level has energy V_{gate}^{eff} with creation (annihilation) operators $\hat{d}^\dagger (\hat{d})$ ³¹. The operators $\hat{c}_{k,\alpha}^\dagger (\hat{c}_{k,\alpha})$ create (annihilate) electrons with momentum k and energy $\varepsilon_{k,\alpha} = E_{k,\alpha} - \mu_\alpha$ in the left ($\alpha = L$) or right ($\alpha = R$) free metallic leads, while the electronic tunneling between the molecular level and a state in the lead has amplitude $V_{k,\alpha}$. The chemical potentials in the leads μ_L and μ_R are assumed to be biased by an external voltage $eV_{bias}^{eff} = \mu_L - \mu_R$. The coupling to the leads is described by the tunneling rate $\Gamma_{\alpha,k} = 2\pi\rho_\alpha |V_{k,\alpha}|^2/\hbar$, where ρ_α is the density of states in the lead α . We will suppose symmetric coupling ($\Gamma_{L,k} = \Gamma_{R,k}$) and a flat density of states for the leads, considered as thermostats at finite temperature, within the wide-band approximation ($\Gamma_{\alpha,k} \mapsto \Gamma_\alpha$, $\alpha = L, R$)^{16,25}.

The Hamiltonian of the mechanical degree of freedom is given by $\hat{H}_{osc} = \frac{\hat{p}^2}{2m} + \frac{1}{2}m\omega_0^2\hat{x}^2$, characterized by the frequency ω_0 and the effective mass m ($k = m\omega_0^2$). The interaction is provided by $\hat{H}_{int} = \lambda\hat{x}\hat{N}_{el}$ ^{24,25}, where λ is the electron-oscillator coupling strength and $\hat{N}_{el} = \hat{d}^\dagger \hat{d}$ represents the electronic occupation on the nanotube (see

also Appendix A). Definitely, the overall Hamiltonian is

$$\hat{\mathcal{H}} = \hat{\mathcal{H}}_{el} + \hat{H}_{osc} + \hat{H}_{int}. \quad (2)$$

In this paper, we will measure lengths in units of $x_0 = \frac{\lambda}{k}$ and energies in units of $\hbar\Gamma$.

The experimental values of the resonance frequencies of the vibrating nanotube (120-300 MHz range) suggest that the vibrational motion is very slow compared to the electronic tunneling rate on the nanotube itself (adiabatic limit): $\omega_0/\Gamma \ll 1$. Moreover, it was estimated in Ref.[25] that for the experiment in consideration the coupling energy describing electron-phonon interaction, $E_p = \frac{\lambda^2}{2k} \simeq 5\mu eV$, implying a strong coupling between the electronic and vibrational degrees of freedom ($E_p/\hbar\omega_0 = 10$). Summarizing, the regime of the relevant parameters is $\hbar\omega_0 \ll E_p (\sim k_B T) \ll eV_{bias}^{eff} \leq \hbar\Gamma$ ²⁷.

As discussed in Ref.[12] and [34], when $eV_{bias}^{eff} \gg \hbar\omega_0$ and $k_B T > \hbar\omega_0$, the semi-classical treatment of the oscillator dynamics is well justified. Within a non-equilibrium adiabatic approximation^{11-13,18,19}, the vibrational dynamics of the nanotube can be described by a *nonstandard Langevin equation* controlled by a self-consistent effective *anharmonic* force as well as by damping and diffusive terms depending explicitly on the resonator displacement x . The oscillator dynamics can be obtained by solving numerically the following equation

$$m\ddot{x} + A(x)\dot{x} = F(x) + \xi(t) + A_{ext} \cos(\omega_{ext}t), \quad (3)$$

where A_{ext} and ω_{ext} represent the amplitude and the external antenna frequency, respectively. Furthermore, in eq.(3), the position-dependent force $F(x)$, damping $A(x)$, and the intensity of the noise $D(x)$, $\langle \xi(t)\xi(t') \rangle = D(x)\delta(t-t')$ (where $\xi(t)$ is a standard white noise term), are related to the electronic Greens functions on the Keldysh contour as^{11,12,18,19},

$$F(x) = -kx + \lambda \langle \hat{N}_{el} \rangle(x), \quad (4)$$

$$\langle \hat{N}_{el} \rangle(x) = \int \frac{d\hbar\omega}{2\pi i} G^<(\omega, x) \quad (5)$$

$$A(x) = \lambda^2 \int \frac{d\hbar\omega}{2\pi} G^<(\omega, x) \partial_{\hbar\omega} G^>(\omega, x), \quad (6)$$

$$D(x) = \lambda^2 \int \frac{d\hbar\omega}{2\pi} G^<(\omega, x) G^>(\omega, x). \quad (7)$$

The lesser $G^<$ and greater $G^>$ Greens functions at finite temperature are given by

$$G^<(\omega, x) = \frac{i\hbar\Gamma}{2} \frac{f_L(\omega) + f_R(\omega)}{(\hbar\omega - V_{gate}^{eff} - \lambda x)^2 + (\hbar\Gamma/2)^2}, \quad (8)$$

$$G^>(\omega, x) = \frac{-i\hbar\Gamma}{2} \frac{2 - f_L(\omega) - f_R(\omega)}{(\hbar\omega - V_{gate}^{eff} - \lambda x)^2 + (\hbar\Gamma/2)^2}, \quad (9)$$

where $f_{L,R}(\omega)$ are the Fermi functions of the leads and we have assumed that $\hbar\Gamma_L = \hbar\Gamma_R = \hbar\Gamma/2$. At low temperatures, $k_B T \ll \hbar\Gamma$, the Fermi function $f_\alpha(\omega)$ can be

replaced by the step function $\Theta(\hbar\omega - \mu_\alpha)$ ($\alpha = L, R$), obtaining

$$\langle N_{el} \rangle(x) = \frac{1}{2\pi} \sum_{\alpha=L,R} \left(\arctan \left(\frac{\mu_\alpha - V_{gate}^{eff} - \lambda x}{\hbar\Gamma/2} \right) + \frac{\pi}{2} \right), \quad (10)$$

$$A(x) = \frac{4m\omega_0}{\pi} \frac{\hbar\omega_0}{\hbar\Gamma} \frac{E_p}{\hbar\Gamma} \sum_{\alpha=R,L} \frac{1}{\left[\left(\frac{\mu_\alpha - V_{gate}^{eff} - \lambda x}{\hbar\Gamma/2} \right)^2 + 1 \right]^2}, \quad (11)$$

$$D(x) = \frac{m\omega_0 E_p}{\pi} \frac{\hbar\omega_0}{\hbar\Gamma} \left\{ \arctan \left(\frac{\mu_\alpha - V_{gate}^{eff} - \lambda x}{\hbar\Gamma/2} \right) + \frac{\frac{\mu_\alpha - V_{gate}^{eff} - \lambda x}{\hbar\Gamma/2}}{\left[\left(\frac{\mu_\alpha - V_{gate}^{eff} - \lambda x}{\hbar\Gamma/2} \right)^2 + 1 \right]} \right\}_{\alpha=L}^{\alpha=R}. \quad (12)$$

The linear elastic force exerted on the oscillator is modified by a relevant *nonlinear* correction term proportional to the electronic occupation eq.(10). The strength of the damping $A(x)$ and diffusive $D(x)$ terms result proportional to the adiabatic ratio ω_0/Γ and therefore one can safely neglect their spatial dependence. Anyway, we point out that the diffusive term $D(x)$ vanishes at equilibrium (bias voltage $V_{bias}^{eff} = 0$). Only on application of finite bias it becomes different from zero. In the regime of experimental parameters explored in Refs. 7 and 8, $\hbar\omega_0 \ll E_p (\sim k_B T) \ll eV_{bias}^{eff} \leq \hbar\Gamma$, the effect of the electronic bath on the resonator dynamics can be described by an effective temperature proportional to the bias voltage $k_B T_{eff} \simeq eV_{bias}^{eff}/8$ ^{11,12}.

In eq.(3), we consider the parameter A_{ext} expressed in terms of the natural force unit $\lambda = \omega_0 \sqrt{2mE_p}$. Assuming a nanotube mass of $m \sim 10^{-23} kg$, an oscillation frequency of 120 MHz, λ is of the order of $10^{-16} N$, while the effective spring constant is $k = 10^{-6} N/m$. By solving the second order stochastic differential equation (3)¹², we are able to obtain the distribution probabilities of the displacement $P(x)$. This allows us to calculate any system property as an average over the distribution probability $P(x)$. In particular, in order to make contact with experimental results, we have calculated the average electronic current $\langle I \rangle$ flowing through the nanotube as $\langle I \rangle = \int_{-\infty}^{+\infty} dx I(x) P(x)$, where $I(x)$ is the current at a particular resonator displacement.

III. RESULTS

One of the main results of Ref. 7 and 8 is the observation of the electronic current changes at fixed gate voltage as function of the external antenna frequency and amplitude. Our model accurately reproduces the experimental results both in a low current-carrying state, where a peak in the current signals a mechanical resonance (Fig.1a),

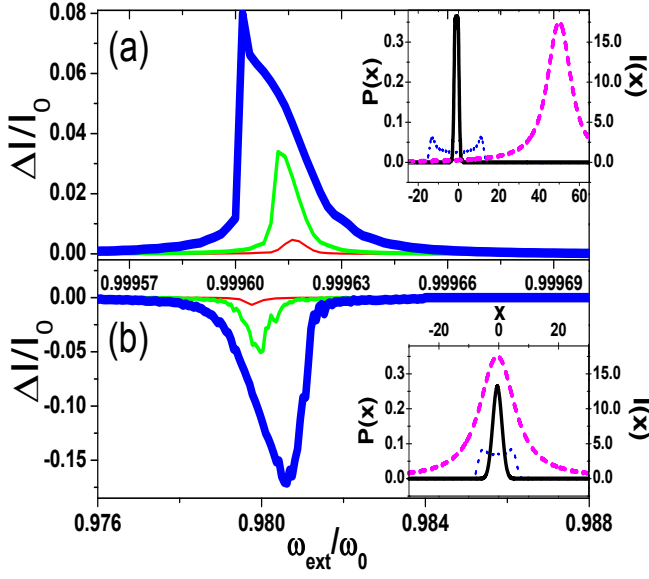


FIG. 1. (Color online) Panel(a): Normalized current change ($\Delta I/I_0$) in a low current-carrying state ($V_{gate}^{eff} = -4\hbar\Gamma$) as function of the external frequency (ω_{ext}/ω_0) for different antenna amplitudes: $A_{ext} = 10^{-5}$ solid thin line (red online), $A_{ext} = 10^{-4.5}$ normal thickness line (green online), $A_{ext} = 10^{-3.5}$ thick line (blue online). Panel (b): $\Delta I/I_0$ against ω_{ext}/ω_0 in a high current-carrying state ($V_{gate}^{eff} = E_p$) for different antenna amplitudes: $A_{ext} = 10^{-3.5}$ solid thin line (red online), $A_{ext} = 10^{-3}$ normal thickness line (green online), $A_{ext} = 10^{-2.5}$ thick line (blue online). Insets: solid line (black online) is a distribution $P(x)$ out of mechanical resonance. Dotted line (blue online) is a distribution obtained at mechanical resonance for the larger value of antenna amplitude considered in main plots of panels (a,b). Short-dashed line (magenta online) represents current as function of position $I(x)$. In this plot $eV_{bias}^{eff} = 0.5\hbar\Gamma$, $\omega_0/\Gamma = 0.004$ and $E_p/\hbar\Gamma = k_B T/\hbar\Gamma = 0.04$.

and in a high current-carrying state, where a dip is observed (Fig.1b).

These two behaviors (peak and dip) can be understood considering that the oscillator explores wider regions in configuration space when the external antenna amplitude increases (see the distribution probabilities $P(x)$ shown in the insets of Fig. 1). When the electronic device is in a low current-carrying state (Fig.1a), $P(x)$ is concentrated at x values far from the configurations where the device carries the maximum current (inset of Fig.1a). By increasing the external antenna amplitude, the resonator is able to explore larger regions which carry more and more current obtaining a positive contribution in the normalized electronic current change $\Delta I/I_0$ with respect to the background value I_0 . On the contrary, when the device is in a high current-carrying state, the distribution probabilities and the current are centered at the same position (inset of Fig.1b). In this case, the effect of the external antenna is to give a negative contribution in the normal-

ized electronic current change $\Delta I/I_0$ (Fig 1b) since, the resonator explores regions of phase space which carry less and less current (inset of Fig. 1b).

The results shown in Fig.1 allow also to characterize the behavior of the resonator in the nonlinear regime. Interestingly, (see Fig.1a), increasing the amplitude of the external forcing, the shape of the current-frequency curves changes. For small antenna amplitudes, a characteristic Lorentzian shape is observed. This is expected for an harmonic oscillator driven by a periodic forcing in the absence of external noise. In fact, even if in mechanical resonance, the oscillator explores only small regions around the stationary point and nonlinear corrections terms of the force $F(x)$ (eq. (4)) do not come into play. At mechanical resonance, only when the amplitude of the external antenna increases, the oscillator explores a larger region in phase space, where the nonlinear terms of the force acting on the oscillator cannot be neglected.

Within our approach, for large antenna amplitudes and in the presence of noise, the current-frequency profiles assume the experimentally observed characteristic triangular shape⁸. Furthermore, a softening is observed when the device is in a low current-carrying state (Fig. 1a), while an hardening in a high current-carrying state is obtained (Fig. 1b). This nonlinear behavior can be understood by analyzing the properties of the force $F(x)$ (eq. 4) around the stationary point. Softening and hardening behavior of the resonance frequency are usually related to the sign of the cubic nonlinear term³⁵. When the device is in a low current-carrying state, indeed, the sign of this term is positive, giving a net softening effect. In a high current-carrying state ($V_{gate}^{eff} = E_p$) and for bias values sufficiently small, the sign of the cubic nonlinear term is negative providing an hardening.

The temperature dependence of the current-frequency profiles, observed in the experiments, exhibits a non-trivial behavior that supports our model. As shown in Fig.2a, for very small temperatures, a triangular shape is found as discussed above. On the other hand, for sufficiently large temperatures, the current-frequency profile turns into Lorentzian shape, characteristic of the linear response regime (Fig.2c). This counterintuitive behavior is determined by a significative reduction of the intrinsic nonlinear terms in the effective force $F(x)$ on the resonator as function of the temperature. Actually, the correction term due the average electronic occupation (eq. (10)) tends to become independent of the resonator displacement x . Furthermore, the broadening of the current-frequency profiles as function of the temperature is produced not only by this effect but also by the growth of the intrinsic damping coefficient $A(x)$ in the Langevin equation eq.(3). Indeed, with increasing temperatures, $A(x)$ increases where resonator dynamics occurs. The temperature dependence of the intrinsic damping $A(x)$ is also responsible for the behavior of the resonator quality factor Q , defined as $I_0/\Delta I_{half-high}$. In the regime where the current-frequency profiles exhibit a Lorentzian shape, we find a power-law of the kind $T^{-0.40}$ ³⁶ that

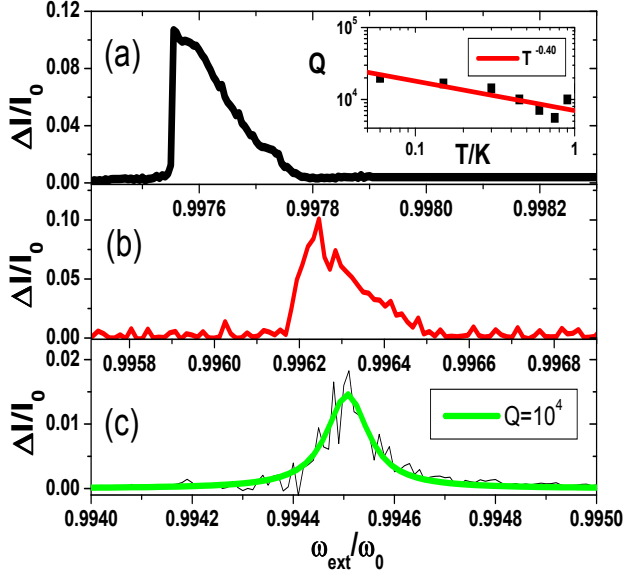


FIG. 2. (Color online) $\Delta I/I_0$ against ω_{ext}/ω_0 in a low current-carrying state ($V_{gate}^{eff} = -1.75\hbar\Gamma$) when the resonator is driven by a strong external antenna amplitude $A_{ext} = 10^{-3.5}$: panel (a) $k_B T = 0.05\hbar\Gamma$, panel (b) $k_B T = 0.375\hbar\Gamma$, panel (c) $k_B T = \hbar\Gamma$. In panel (c) a Lorentzian fit is also drawn with $Q = 10^4$ (Q is defined in the main text). Inset of panel (a): intrinsic quality factor Q as function of temperature³⁶. We use as energy unit $\hbar\Gamma = 125\mu\text{eV}$. In this plot $eV_{bias}^{eff} = 0.5\hbar\Gamma$, $\omega_0/\Gamma = 0.005$ and $E_p/\hbar\Gamma = 0.05$.

is quite close to that found in the experiment ($T^{-0.36}$). However, it is important to point out that this exponent depends on the gate voltage effectively applied to the device.

Finally, we have analyzed all the traces of current variations as function of the antenna frequency, obtained tuning the effective gate voltage. Going from a low to a high current-carrying state, the characteristic dip of the resonance frequency as function of the effective gate voltage is obtained in excellent agreement with experiments (curve (1) of Fig.3). The observed renormalization of the resonance frequency can be related to strong variations of the electronic occupation eq.(10) as function of the gate voltage (see solid line in the inset of Fig.3). When the device is in a low current-carrying state ($|V_{gate}^{eff} - E_p| > 1.5\hbar\Gamma$), the average electronic occupation is not sensitive to gate voltage variations. Instead, in a high current-carrying state ($|V_{gate}^{eff} - E_p| < 1.5\hbar\Gamma$), the electronic occupation shows a strong variation, providing the softening of the resonance frequencies. Increasing the bias voltage to values closer to $\hbar\Gamma$ or larger (line (3) and (4) of Fig. 3), one obtains a broadening of the resonance frequency dip, owing to a wider conduction window with respect to the broadening ($\sim \hbar\Gamma$) of the electronic energy level. Actually, with increasing the bias, the electronic contribution to the effective spring constant increases, producing a nontrivial renormalization of the resonance frequency as

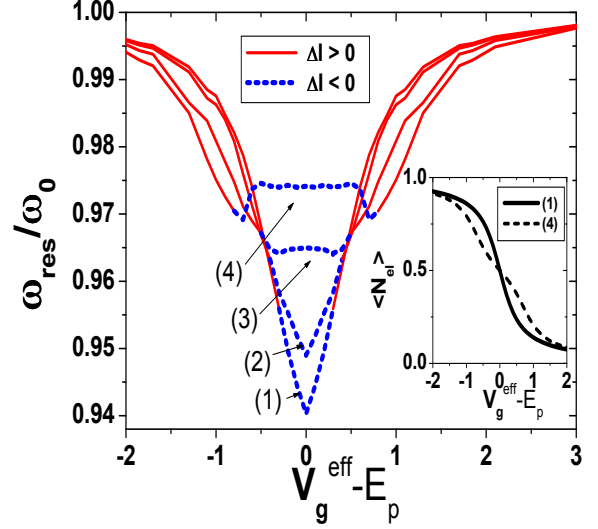


FIG. 3. (Color online) Resonator frequency at resonance against effective gate voltage (shifted of E_p) for different bias voltages: $eV_{bias} = 0.1\hbar\Gamma$ curve (1), $eV_{bias} = 0.5\hbar\Gamma$ curve (2), $eV_{bias} = 1.0\hbar\Gamma$ curve (3), $eV_{bias} = 1.5\hbar\Gamma$ curve (4). Solid (red online) and short-dashed (blue online) portions of each curve indicate resonance frequency values with positive and negative current change ΔI , respectively. Inset: electronic occupation at resonance frequency against effective gate voltage (shifted of E_p) for $eV_{bias} = 0.1\hbar\Gamma$ (curve (1)) and $eV_{bias} = 1.5\hbar\Gamma$ (curve (4)). In this plot $A_{ext} = 10^{-3}$, $\omega_0/\Gamma = 0.01$ and $E_p/\hbar\Gamma = k_B T/\hbar\Gamma = 0.1$.

function of the gate. We note that for $eV_{bias}^{eff} = 1.5\hbar\Gamma$ (line (4) of Fig. 3), a fine structure represented by two very small dips appears. When the bias window, whose extension is proportional to eV_{bias}^{eff} , becomes larger than the broadening of the level, one could tune the electronic device into a region of conducting states where the variations of the occupation are smaller than that obtained at the boundary of the conduction window itself (see dashed line in the inset of Fig.3). When the electronic device goes through states with different conducting character, the maximum renormalization of the resonance frequency occurs, providing two dips in the resonance frequency of the nanotube. This feature could be experimentally observed with a larger resolution in the applied gate voltage, when a very large bias is applied to the nanotube.

IV. CONCLUSIONS

In conclusion, we have studied a self-detecting SET realized by a suspended carbon nanotube including, in a non-perturbative way, the effect of the antenna driving the nanotube toward a nonlinear regime. All the qualitative features of the device, experimentally observed, are accurately reproduced clarifying the origin of the nonlin-

ear effects. The nonlinear behavior is understood without adding *by hand* nonlinear terms to the effective force exerted on the resonator^{7,16,25,28}, but stems out naturally from the nontrivial nonequilibrium time-dependent electronic occupation controlled by the coupling with the leads. We have shown that, increasing the temperature, the nonlinear effects in the current-frequency response are washed out as a result of the increase of the intrinsic damping of the resonator and of the reduction of the intrinsic nonlinear terms of the effective self-consistent force. Within our approach, a broadening of the frequency dip as function of the bias voltage is reproduced, predicting in the limit of large bias a double dip structure.

V. ACKNOWLEDGMENTS

A. Nocera acknowledges G. A. Steele for very useful clarifications and CNISM for the financial support.

Appendix A

Here, we briefly show that the model Hamiltonian for the vibrating nanotube encapsulated in the eq.(2) is equivalent to that used in^{7,8} and in other papers in the literature^{20–23,25,30}. Indeed, as clearly discussed in Ref. 32, a single electronic transistor (SET) consists of a metallic dot (represented by a nanotube in the case considered in Ref. 7 and 8) with a large Coulomb-charging energy $E_C = e^2/2C_{tot}$ (C_{tot} is the total capacitance of the dot) coupled via tunnel junctions to both a source and a drain metal electrode. The Hamiltonian for the electronic and vibrational degrees of freedom of the dot is given by

$$H_{dot} = E_C(N_{el} - N_{gate})^2 + \frac{1}{2}kx^2, \quad (A1)$$

comprising a charging-energy term and the harmonic vibrational energy. In eq.(A1), N_{el} is the charge on the

SET dot and $N_{gate} = C_{gate}V_{gate}/e$ is the dimensionless electron number associated with a gate voltage V_{gate} which is coupled to the dot via a capacitance C_{gate} . In addition, a voltage V_{bias} is applied between source and drain which drives the tunneling of electrons across the SET. Here, $C_{tot} = C_{gate} + C_{leads}$, where C_{leads} is the sum of the capacitances resulting from the coupling to the leads. When the nanotube is allowed to vibrate, the gate capacitance C_{gate} assumes a spatial dependence $C_{gate}(h(x))$, where h is the distance between the nanotube and the gate electrode when the nanotube is displaced by a distance x from its equilibrium position ($h(x) = h_0 + x$). In the limit of small displacements, one can expand $\hat{H}_{dot}(x)$ around $x = 0$ obtaining a Holstein-like linear correction term in x :

$$H_{int} = \lambda N_{el}x, \quad (A2)$$

where $\lambda = -2(E_C V_g/e)(dC_g/dx)$. In the small energy window of interest for a single dip feature investigated in Ref. 7 and 8, we can neglect the weak gate and bias voltage dependence of λ that is assumed constant^{21,32,33}. Moreover, if we choose $x = 0$ as the position where the Coulomb force for $N_{el} = 0$ electrons in the island equals the elastic force, λ can be then interpreted as the net force acting on the nanotube when one excess electron is populating the nanotube itself. The terms independent on N_{el} in the above expansion are usually neglected^{32,33}. One further assumes that the gate voltage is such that only charge states with $N_{el} = 0$ and 1 are accessible. In this case, $N_{el}^2 = N_{el}$ and one can incorporate remaining constant terms (independent on x) in the above expansion in an effective gate voltage obtaining

$$H_{dot} \simeq V_{gate}^{eff} N_{el} + \lambda N_{el}x + \frac{1}{2}kx^2. \quad (A3)$$

If we quantize the electronic and vibrational degrees of freedom, eq.(A2) gives the Holstein coupling discussed in the main text.

¹ B. Witkamp, M. Poot, and H. S. J. van der Zant, *Nano Lett.* **6**, 2904 (2006).

² H. G. Craighead, *Science* **290**, 1532 (2000).

³ K. L. Ekinci, M. L. Roukes, *Rev. Sci. Instrum.* **76**, 061101(2005).

⁴ M. D. LaHaye, O. Buu, B. Camarota, and K. C. Schwab, *Science* **304**, 74 (2004).

⁵ K. C. Schwab, M. L. Roukes, *Phys. Today* **58**, 36 (2005).

⁶ A. D. O'Connell, M. Hofheinz, M. Ansmann, R. C. Bialczak, M. Lenander, E. Lucero, M. Neeley, D. Sank, H. Wang, M. Weides, J. Wenner, J. M. Martinis, and A. N. Cleland, *Nature* **464**, 697 (2010).

⁷ G. A. Steele, A. K. Huttel, B. Witkamp, M. Poot, H. B. Meerwaldt, L. P. Kouwenhoven, and H. S. J. van der Zant,

Science **325**, 1103 (2009).

⁸ A. K. Huttel, G. A. Steele, B. Witkamp, M. Poot, L. P. Kouwenhoven, and H. S. J. van der Zant, *Nano Lett.* **9**, 2547 (2009).

⁹ Usually, increasing the temperature, one would expect to access the region far away the potential minimum, where nonlinear effects could be present.

¹⁰ For the sake of simplicity, back-actions effects of the vibrating resonator on the electromagnetic field of the antenna are disregarded.

¹¹ D. Mozysky, M. B. Hastings, and I. Martin, *Phys. Rev. B* **73**, 035104 (2006).

¹² A. Nocera, C. A. Perroni, V. Marigliano Ramaglia, and V. Cataudella, *Phys. Rev. B* **83**, 115420 (2011).

- ¹³ J. Splettstoesser, M. Governale, J. König, and R. Fazio, *Phys. Rev. Lett.* **95**, 246803 (2005).
- ¹⁴ N. Bode, S. V. Kusminskiy, R. Egger, and F. von Oppen, *Phys. Rev. Lett.* **107**, 036804 (2011).
- ¹⁵ N. Bode, S. V. Kusminskiy, R. Egger, and F. von Oppen, *Beilstein J. Nanotechnol.* **3**, 144 (2012).
- ¹⁶ G. Weick, and Dominique M.-A. Meyer, *Phys. Rev. B* **84**, 125454 (2011).
- ¹⁷ A. Metelmann, and T. Brandes, *Phys. Rev. B* **84**, 155455 (2011).
- ¹⁸ F. Pistolesi, Ya. M. Blanter, and I. Martin, *Phys. Rev. B* **78**, 085127 (2008).
- ¹⁹ R. Hussein, A. Metelmann, P. Zedler, and T. Brandes, *Phys. Rev. B* **82**, 165406 (2010).
- ²⁰ G. Labadze and Ya. M. Blanter, arXiv1007.5186v2 (2010).
- ²¹ S. D. Bennett, L. Cockins, Y. Miyahara, P. Grutter, and A. A. Clerk, *Phys. Rev. Lett.* **104**, 017203 (2010).
- ²² Ya. M. Blanter, O. Usmani, and Yu. V. Nazarov, *Phys. Rev. Lett.* **93**, 136802 (2004).
- ²³ Ya. M. Blanter, O. Usmani, and Yu. V. Nazarov, *Phys. Rev. Lett.* **94**, 049904(E) (2005).
- ²⁴ A. D. Armour, M. P. Blencowe, and Y. Zhang, *Phys. Rev. B* **69**, 125313 (2004).
- ²⁵ G. Weick, F. von Oppen, and F. Pistolesi, *Phys. Rev. B* **83**, 035420 (2011).
- ²⁶ In sequential tunneling regime, $\hbar\Gamma \ll \min[eV_{bias}, k_B T]$, the tunneling events between the leads and the molecule are energy-conserving, with the rates determined by Fermi's golden rule at the lowest order in perturbation theory in the tunneling Hamiltonian $\hat{H}_{tun} = \sum_{k,\alpha} (V_{k,\alpha} \hat{c}_{k,\alpha}^\dagger \hat{d} + h.c.)$. In the cotunneling regime, $eV_{bias} < \hbar\Gamma < k_B T$ or $k_B T < \hbar\Gamma < eV_{bias}$ or $\max[eV_{bias}, k_B T] < \hbar\Gamma$, higher-order tunneling events become dominant.
- ²⁷ It is very difficult to infer the actual values of the effective source-drain bias eV_{bias}^{eff} and the gate voltage V_{gate}^{eff} applied to the device from the experimental setup. Due to the capacitive coupling between the carbon nanotube and the surrounding electrodes and to the length (400 – 1100nm) of the nanotube itself, only a fraction of the applied bias and gate voltage acts effectively onto the nanotube level interested in the transport^{7,8}.
- ²⁸ S. Ramakrishnan, Y. Gulak, and H. Benaroya, *Phys. Rev. B* **78**, 174304 (2008).
- ²⁹ T. Holstein, *Ann. Phys. (N.Y.)* **8**, 325 (1959).
- ³⁰ N. Traverso Ziani, G. Piovano, F. Cavaliere, and M. Sassetti, *Phys. Rev. B* **84**, 155423 (2011).
- ³¹ We consider for simplicity spin-less electrons, as the inclusion of spin as well as on-site Coulomb repulsion doesn't qualitatively change our results.
- ³² A. A. Clerk and S. Bennett, *New J. Phys.* **7**, 238 (2005).
- ³³ F. Pistolesi and S. Labarthe, *Phys. Rev. B* **76**, 165317 (2007).
- ³⁴ A. Mitra, I. Aleiner, and A. J. Millis, *Phys. Rev. Lett.* **94**, 076404 (2005).
- ³⁵ A. H. Nayfeh and D. T. Mook, *Nonlinear oscillations* (Wiley Classics Library Edition, 1995).
- ³⁶ We have verified that, in the range of temperature investigated ($0.05 < k_B T / \hbar\Gamma < 1 \rightarrow 60mK < T < 1.2K$), the widths of current frequency profiles are independent on the external antenna amplitude applied to tune the resonator in the linear response regime.